HHS Public Access

Author manuscript

Nanoscale. Author manuscript; available in PMC 2017 November 10.

Published in final edited form as:

Nanoscale. 2016 November 10; 8(44): 18718–18725. doi:10.1039/c6nr06235k.

Active modulation of drug release by ionic field effect transistor for an ultra-low power implantable nanofluidic system

Giacomo Bruno[a,b,†], **Giancarlo Canavese**[c,†], **Xuewu Liu**[a], **Carly S. Filgueira**[a], **Adriano Sacco**[d], **Danilo Demarchi**[b], **Mauro Ferrari**[a], and **Alessandro Grattoni**[a]

[a]Department of Nanomedicine,Houston Methodist Research Institute, 6670 Bertner Avenue, Houston, TX 77030, USA

[b]Department of Electronics and Telecommunications, Politecnico di Torino, Corso Duca degli Abruzzi 24, Turin 10129, Italy

[c]Department of Applied Sciences and Technology, Politecnico di Torino, Corso Duca degli Abruzzi 24, Turin 10129, Italy

[d]Center for Sustainable Futures @POLITO, Instituto Italiano di Tecnologia, Corso Trento 21, Turin 10129, Italy

Abstract

We report an electro-nanofluidic membrane for tunable, ultra-low power drug delivery employing an ionic field effect transistor. Therapeutic release from a drug reservoir was successfully modulated, with high energy efficiency, by actively adjusting the surface charge of slit-nanochannels 50, 110, and 160 nm in size, by the polarization of a buried gate electrode and the consequent variation of the electrical double layer in the nanochannel. We demonstrated control over the transport of ionic species, including two relevant hypertension drugs, atenolol and perindopril, that could benefit from such modulation. By leveraging concentration-driven diffusion, we achieve a 2 to 3 order of magnitude reduction in power consumption as compared to other electrokinetic phenomena. The application of a small gate potential (±5 V) in close proximity (150 nm) of 50 nm nanochannels generated a sufficiently strong electric field, which doubled or blocked ionic flux depending on the polarity of the voltage applied. These compelling findings can lead to next generation, more reliable, smaller, and longer lasting drug delivery implants with ultra-low power consumption.

Introduction

Active control of molecular transport is fundamental for mimicking the physiological regulation of chemicals across cell membranes, tissues, and in complex biological systems. Living organisms rely on cyclic phenomena which are essential for numerous biological processes.[1] These biological clocks have a substantial impact on the pathophysiology of diseases, as well as the efficacy of therapeutic regimens. In cardiovascular disease,

[†]Equal contribution

Electronic Supplementary Information (ESI) available. See DOI: 10.1039/x0xx00000x

preventative treatments, such as administration of β-blockers can reduce risk; however, too large a dose can result in complications like difficulty breathing and irregular heartbeats. Early intervention with therapeutics, such as atenolol, in acute myocardial infarction can reduce infarct size and decrease mortality; nonetheless, when usage is discontinued, its dosage must be reduced gradually since abrupt stoppage may worsen angina or precipitate a heart attack.[2] Perindopril, another therapeutic administered for hypertension, requires cautious dosage adjustments in accordance with creatinine clearance as renal failure is a potential complication.[3] In light of this, there is a growing interest in the development of novel biomimetic devices capable of the tunable and timed-manipulation of analytes, as is the case for controlled drug delivery systems. Examples of these efforts are the works of Langer,[4] Cima,[5] de Rooij,[6] among others on implantable technologies for the tunable administration of therapeutics. Despite significant advances in the field,[7] the current state of the art consists of high energy consumption devices[8] requiring bulky batteries[9] that set strict limitations on their lifespan and potential applications. Large power consumption and, in turn, large batteries, result in drawbacks such as health risks due to stored charge and size limitations, which place surgical restrictions on implantation where there is physiologically limited space (i.e. treatment of pathologies related to eye, ear, and nose). Moreover, large batteries may require larger surgical incisions, resulting in aesthetic problems or infections, increased pressure or friction on adjacent tissues, and can decrease efficiency as the mass implanted may be large, but delivers a small drug payload. The reduction in power consumption required to advance implantable devices can be analogous to the downscaling of integrated circuits in the semiconductor industry; a necessary advancement that could accelerate the clinical development of implantable delivery systems. Modern medicine would significantly benefit from technologies that expand approaches to drug administration and dosage modulation over time.

Electrofluidics, leveraging electrokinetics in nanofluidic systems, may offer a valid solution for reducing energy consumption of drug delivery devices while increasing their energy efficiency. Charged particles or molecules can be efficiently sorted, displaced, and manipulated, through nanochannels by leveraging a variety of physical phenomena including electroosmosis, electrophoresis, and ionic concentration polarization.[10,11] Unlike mechanical pumping devices, electrofluidic systems demonstrate high efficiency in electrical-to-mechanical energy conversion,[12–14] and remain robust due to a lack of complex moving mechanisms potentially subject to failure.[15–17] As such, electrofluidics have been adopted in various applications such as sensors,[18–20] displays,[21] and biological sample analysis and manipulation.[22–24] Within the field of electrofluidics, proof of concept electrophoretic and electroosmotic delivery devices have been shown.[25] Both electrophoresis and electroosmosis, however, suffer from intrinsic energy losses related to fluid conductivity, channel geometry, and viscous effects on molecular transport within fluids or fluids within channels.

Electrostatic modulation of concentration-driven diffusive transport introduces a potential strategy for controlling molecular transport with minuscule energy consumption. Several works have shown how charged silica nanochannels can be used to passively achieve controlled drug delivery, both *in vitro*[26–29] and *in vivo*[30–32], by physical and electrostatic nanoconfinement on molecules diffusing out from an implantable reservoir. The silica walls

(resulting from oxidation of the silicon surface to form silicon dioxide, yielding a negative interface charge) attract positive molecules,[33] termed counter-ions, and repel negative ions, named co-ions, which leads to an ionic redistribution of charges across channels and generates passive release regimes such as near-surface or gated diffusion.[26]

By changing the surface charge, it is possible to leverage new electrofluidic phenomena and obtain electronic-like components, such as diodes and transistors.[34–36] Other researchers have demonstrated the ability to tune nanochannel properties (such as surface charge, size, and hydrophobicity) utilizing different approaches that include chemically functionalizing nanochannels with polymers[37] and proteins,[38,39] or by changing the pH of the solution.[40,41] Alternatively, similar results can be achieved by applying *ad hoc* a reversible strong electric field (approximately 10^6 V/m) to polarize the channels with the preferred charge,[35,42] resulting in a simpler and more versatile strategy to achieve modulation. Control over the potential of the nanochannel through the use of a nearby gate electrode is advantageous as it is both an effective and reversible technique. In fact, properly insulated gate electrodes are associated with negligible leakage currents and low power consumption. Yet, the majority of researchers exploiting this effect are focusing on modeling and utilizing electrokinetic flow (applying a potential between source and drain)[43–45] to better understand basic transport mechanisms. Here, we demonstrate that it is possible to leverage passive ionic diffusion modulated solely by an isolated gate electrode (theoretically without any associated energy consumption), and apply its use for drug delivery systems.

Materials and Methods

In this work, we investigated the use of a gate potential for the ultra-low power modulation of drug release from a silicon nanochannel delivery system (Figure 1). Silicon membranes presenting a parallel set of 100 slit-nanochannels were microfabricated using a sacrificial-oxide technique to obtain channels with 50, 110, and 160 nm nominal size. AFM characterization yielded a measured averaged size of 56±1, 119±2.5, and 159±2.5 nm, respectively (see Supporting Information). Gate electrodes were created within pyrex 7740 capping wafers using a trench method. Briefly, electrodes were patterned on the pyrex using photolithography on an EVG 620 aligner. 500 nm trenches were obtained by CF_4-based reactive ion etching. A Ti-Au-Ti sandwich layer (20/100/30 nm) followed by a 350 nm Pyrex layer was deposited in the trench using a CHA E-Beam Evaporator. After removing the photoresist, chemical mechanical polishing was used to refine the surface, prior to bonding the pyrex layer onto the silicon substrate. While, details of the device fabrication including the silicon substrate are provided in the Supporting Information, additional details concerning the general fabrication approach can be found in Grattoni *et al.*[16] We chose to examine the transport of two different commonly prescribed hypertensive drugs: atenolol (+1q charged at neutral pH) and perindopril (−1q charged at neutral pH) across our nanofluidic device as an initial proof of concept. Their release was actively modulated utilizing both ultra-low power consumption (diffusion driven transport, modulated by the gate voltage) with or without a Drain-Source voltage. By exploiting these two different conditions, we could measure and compare energy consumption and maintain better control over the charge distribution along the nanochannels.

Results and Discussion

Characterization and Choice of Membrane

Prior to initiating drug release experiments, we sought to measure transmembrane current by applying a potential, also referred to as the Drain-Source voltage (V_{DS}), between the inlet and outlet of the nanochannels to aid in our evaluation of electrokinetic energy consumption. V_{DS} was used as the primary source driving ion transport (e.g. K^+ and Cl^-). The resulting ionic flux was modulated by a secondary electric field, generated by the gate potential (V_G), and applied by a buried gate electrode placed in proximity to the nanochannel surface as represented in Figure 1b. When a potential was applied to this electrode, a rearrangement of local ions was forced by the new electric field. The described system is very similar to a field effect transistor (FET), with the only difference being that the gate voltage, instead of modulating the drain-source *electric* current, regulates the drain-source *ionic* flux. In this fluidic system, co-ions and counter-ions replace the role of electrons and holes in an equivalent electrical system, resulting in an ionic field effect transistor (IFET). To the best of our knowledge, these results represent the first use of an IFET as a drug delivery regulator with the ability to be implanted *in vivo* due to its bioinert construction as well as low energy consumption, therefore, requiring a minimal battery compartment.

In order to determine which device configuration would be the most suitable for modulating the transport of charged molecules, we performed preliminary experiments on 50, 110, and 160 nm nanochannel membranes with 1 mM KCl electrolyte solution present at both the inlet (inside the drug reservoir) and outlet (sink solution) to prevent salt diffusion in the absence of an applied voltage and measured the drain-source current for different applied gate voltages. The results (shown in Figure 2) exhibit a directly polarized diode-like trend for the larger membranes (Fig. 2b and c), since large currents are measured when a certain voltage threshold is surpassed. As reported by Vermesh *et al.*[14] in positively charged nanochannels, this current flux is due to a change in transport from no slip to slip flow. In the no slip condition, there is no flux of ions in proximity to the nanochannel walls due to the adhesion of counter-ions with the charged silica surface, increasing the drag and resistivity. In this approximation, the flux depends on channel size (diffuse-layer thickness), zeta potential of the channel walls, and ionic strength.[46] Slip transport, on the other hand, is when sufficient potential is applied, and the ions belonging to the Stern layer can be moved tangentially to the channels' surfaces, electroosmotically pulling water with them and thereby drastically increasing the measured current. With the 50 nm nanochannel device, this phenomenon does not occur due to the larger ratio between the Debye length and the nanochannel height. Despite this, a similar trend can be seen for all three nanochannel sizes: higher current when a negative gate voltage is present, and minimal current when a positive gate voltage is applied.

We chose to perform the following experiments with 50 nm nanochannel substrates, where the no slip condition (low drain-source current values) presides because we noted remarkably high currents for the larger size nanochannels. These high currents seem to be consistent with the slip condition of electroosmotic flow, which correlate with a non-linear increase in energy consumption. Therefore, to minimize device power consumption, we

avoided the slip condition, characterized by high drain-source current, by using the 50 nm membranes. Due to this non-linearity, to properly tune the drug release rate one should modify nanochannel number as opposed to increasing nanochannel size.

Conductance and Transport Analysis

Figure 3a shows the variation in conductance for the 50 nm nanochannel device using KCl as the electrolyte solution at different gate voltages, ranging from −10 V to +10 V, and different ionic concentrations. The solution ionic concentration, ranging from 10 μM to 100 mM, was replaced for both the drug and sink reservoirs, impeding the creation of any unwanted ionic concentration diffusion. The data displayed a conductance trend that could be effectively qualified by the Geometry-Governed-Conductance (GGC) equation:[47]

$$\frac{1}{V}=2F\mu\sqrt{\left(\frac{\sum}{2}\right)^2+C_0^2}\cdot\frac{wh}{l} \quad (1)$$

where F is Faraday's constant (C mol^{-1}), μ is the ionic mobility (m^2 s^{-1} V^{-1}), Σ is the molar concentration of ions in the nanochannel volume (mol L^{-1}), C_0 is the molarity of the solution (mol L^{-1}), and w, h, and l are respectively the width, height, and length of the channel (m). The equation describes the conductance (I/V) of the system as a function of Σ, and therefore, by measuring the solution resistance at a particular concentration, one can estimate the number of ions within the nanochannel. Use of the GGC equation and model also allows for predictive results when direct measurements of the nanochannel properties may not be feasible, such as surface charges, ion concentration or distribution. The dashed line represented in Figure 3a was obtained by considering $\Sigma=\sigma\cdot wl/wlh$ where the surface charge (σ) was equal to −0.06 C/m^2, as reported in previously conducted studies[26,48] in electroneutral conditions and is good agreement with the collected data without any gate potential applied.

The case of negative gate potential

Interesting results arise when a negative gate potential is applied, as a great increase in conductivity (one order of magnitude greater than our other measurements) was observed. These measurements, in agreement with the current curves represented in Figure 2, denote that a greater number of positive ions must reside in proximity to the gate electrode region to assure overall nanochannel electroneutrality. At low ionic strength (Figure 3b), this current is mostly composed of positive ions in the nanochannels, as negative molecules are strongly repelled by a large Debye length. The positive counter-ions are thereby transported across the uniformly charged surface in the Stern layer, and their concentration is strongly dependent on the applied gate voltage. At high ionic strength (Figure 3c), the Debye length is remarkably shortened and the charge transport though the nanochannels is severely affected by two different contributing regions: bulk and surface. The bulk of channel allows for charge transport of both positive and negative ions migrating in opposite directions regardless of the gate voltage. Near the channel surfaces the negative electric field generated by the gate electrode results in a proportional increase in counter-ions, which consequently increase conductivity.

The case of positive gate potential

When a positive gate potential was applied a reduction in conductivity was measured for a solution with low ionic concentration (less than 1 mM KCl). The presence of a positive electric field prevents the passage of the positively charged ions, which are the major carrier of the electric current in conditions of low ionic strength (Figure 3d). In fact, the local ion rearrangement induces a depletion of positive ions in the gate region, resulting in an increased energetic penalty for cations to travel across the nanochannel system. This drastic variation in ionic concentration near the gate region may be visualized as an ionic discontinuity. The discontinuity only presides at low ionic strength, where relatively large Debye lengths predominate, rendering the nanochannels highly ion selective. At higher ionic strength (Figure 3e) and relatively small Debye length, it is possible for negative ions to enter the nanochannels and participate in current transport. In this case, the application of a positive gate potential is irrelevant because both charges can pass through without energetic penalty and no discontinuity arises. Adjacent to the negative ions, which attract due to the positive gate, a layer of positive ions accumulates to form an electric double layer. This explains well why in condition of high ionic strength (greater than 1 mM KCl) the conductivity measured does not vary irrespective of the presence of a positive gate voltage.

Nanochannels conductivity and rectification factor

Figure 4a represents the conductance variation across 50 nm nanochannels for different KCl concentrations at both sides of the nanochannels and gate voltages. Normalization of the results at the same molarity leads to a clear visualization of three different regions. A strong increase in current independent of solution molarity, depicted by a continuous bright area (region I in Figure 4), is homogeneously present when a negative voltage is applied. A direct correlation is observed between the amplitude of the negative gate voltage and an increase in conductance. Next to this region presides a dark area, where an applied positive potential solely leads to a decrease in conductivity. At low ionic strength (with concentrations below 1 mM KCl), the Debye length is remarkably amplified, and the nanochannels are mostly permeable to positively charged ions. In this condition, due to the lack of negative ions in proximity to the gate electrode, the counter-ions are strongly repelled from center of the nanochannel. This repulsion leads to a depletion of ions in the gate electrode area, resulting in an ionic discontinuity that increases the electric resistance. The third rectification factor, calculated as the ratio between forwards and reversed bias currents measured at +5 and −5 V_{DS}, was proposed by Guan *et al.*[49] as an effective method for the representation of the variation in conductivity of an IFET. When the reversed bias current is much greater than the forward current, the absolute value of the rectification factor approaches zero, shown as the dark blue region of figure 4b. The graph presents a remarkable peak and valley when the membrane is immersed in a 1 mM KCl solution. This phenomenon can be explained by calculating the ionic flux of ions and their distribution within the channel. If the ions are mostly present in the bulk, in condition of high ionic strength (greater than 10 mM KCl), the transport of current is less affected by the gate electric field. Alternatively, when the ionic strength of the solution is very low (less than 1 mM KCl), the rectification factor is compromised by the lack of negative ions within the channel. In this case, the near surface current supported by positive ions can flow both ways as a function of applied voltage. At

intermediate concentrations (around 1 mM), the transport of a transitional phase is governed by a profound rectification effect.

The described behavior is due to a variation of the nanochannels conductance while a positive or a negative drain-source voltage is applied. When an accumulation region is established in the nanochannel, an increase in conductance is observed, while a depletion condition implies a reduction in conductivity. This variation in conductance is caused by a local and marked disparity in ionic concentration (an increase in concentration of ions with an opposite polarity with respect to the gate potential) in the gate region. To uphold the Kirchhoff current law, an accumulation or depletion effect is established (for $V_G<0$ and $V_{DS}<0$ and for $V_G>0$ and $V_{DS}>0$ depletion occurs, while for $V_G<0$ and $V_{DS}>0$ and for $V_G>0$ and $V_{DS}<0$ accumulation occurs). This rectification factor, which only occurs at intermediate concentration (Figure 4b), is responsible for the increase in conductance area reported in Figure 4a for a positive gate potential, thereby characterizing this region as the one most promising for active control of therapeutic release.

Modulation of Drug Transport

As proof of concept, two charged therapeutics with similar chemical structures and size were chosen to test release modulation due to variation in the ionic field effect controlled by the gate electrode. Atenolol is a positively charged molecule (+1q at neutral pH) with a small mass (266 Daltons) and a calculated volume of 261 $Å^3$.[50] Its role as a beta-blocker is widely used to reduce chest pain and high blood pressure,[51,52] and it can reduce the risk of death after a heart attack. When examining its passive release (0 V_{DS} applied), the presence of a negative gate potential can lead to a 150% increase in transport, while a positive gate voltage reduces the flux by a 40% (Figure 5a). By synergizing the effect with the addition of a drain-source electric field, a greater number of permutations can be tested. For example, when a positive V_{DS} is present, the drug molecules tend to cross the membrane faster, which can be further helped by a negative gate potential. Alternatively, this phenomenon can be antagonized by the repulsive positive gate field, resulting in a decrease of drug released as illustrated in Figure S4. Symmetrically opposite results were obtained with perindopril, a negatively charged drug (−1q at neutral pH). Perindopril (368 Daltons) is 360 $Å^3$ in volume[50] and plays a very similar role in lowering blood pressure and reducing the risk of death for patients with heart problems.[3,51] Its release (Figure 5b) can be modulated effectively with ultra-low power consumption, doubling the flux when a positive gate is present and reducing it to one-fifth the release when the opposite voltage is applied. In addition, the application of a negative drain-source voltage balanced the effect of the negative gate voltage, yielding comparable results to the release rate of the passive reference system.

Energetic Considerations

By monitoring the current during the drug release, it is possible to calculate the power consumption while different voltages are present. A pure electrokinetic flow generated solely by a drain-source voltage consumes between 10 and 100 μWh, while a passive diffusion modulated by the gate electrode is limited between 1 and 5 μWh; thereby, allowing the same battery to last much longer. The combination of both transport phenomena

increases the drain of current, especially when the applied gate voltage is negative. In this worst-case scenario, it is possible to measure an energy request of 1 mWh due to the increase of conductivity of the nanochannels. On the other hand, when a positive voltage is applied the energy request is less (0.4 mWh). This energetic difference is due to the presence of negative charges on the nanochannels surfaces that oppose the generation of a positively charged field, therefore increasing the channel resistance. Both of these are overestimated values, as they are calculated based on several components: gate electrode leakage current, drain-source current induced by the application of an electrical potential V_{DS}, and an ionic current supported by diffusive effect. The most effective modulation was obtained both for atenolol and perindopril with the configuration $V_{DS}=0$ and $V_G=-5$ with an efficiency of about 1 mg/h/(Wh) per nanochannel. Presently, a high nanochannel density of 100,000 nanochannels/mm^2 can be easily fabricated,[16,53] resulting in an increase of drug release and minimal increase of gate leakage current proportional to the channel number. The consequences of this ultra-low power consumption are significant, especially for the active implantable device industry where battery volume comprises a majority portion of the system. The use of ultra-low power systems that leverage passive diffusion could theoretically operate without the need for a battery, for example receiving energy only from a supercapacitor remotely rechargeable by inductive coupling.

Conclusions

In conclusion, we have characterized 50, 110, and 160 nm nanochannels embedded in silicon membranes as an ionic field effect transistor. The presence of an insulated gate electrode placed in close proximity to the nanochannels leads to noticeable variation in the conductance of the system with minimal power consumption (on the order of μWh). As a proof of concept, the release of two charged therapeutics was modulated by the application of two electric fields, confirming the feasibility of a system for the precise control of ionic flux. In addition, drug flow was manipulated in ultra-low power mode by applying only a gate voltage, resulting in currents three orders of magnitude smaller than the one measured when a drain-source voltage is present. These compelling results could lead to new reliable implantable devices with ultra-low power consumption for controlled drug release. Pharmacologic modulation, as demonstrated in this study for perindopril and atenolol, may offer individualized therapy to enhance bioavailability, preserve efficacy, and reduce toxicity.

Supplementary Material

Refer to Web version on PubMed Central for supplementary material.

Acknowledgments

We thank Zongxing Wang for his support with membrane fabrication. Elena Riscaldina and Celeste Marcato for support in experimental study. The work received financial support from the CASIS (GA-14-145) and NIH NIGMS R21 GM 111544.

Notes and references

1. Hess B, Boiteux A. Annu Rev Biochem. 1971; 40:237–258. [PubMed: 4330578]
2. Faulx MD, Francis GS. Curr Probl Cardiol. 2008; 33:703–768. [PubMed: 19000586]

3. The Lancet. 2003; 362:782–788.
4. Santini JT, Cima MJ, Langer R. Nature. 1999; 397:335–338. [PubMed: 9988626]
5. Shawgo RS, Grayson AC Richards, Li Y, Cima MJ. Curr Opin Solid State Mater Sci. 2002; 6:329–334.
6. Receveur RAM, Lindemans FW, de Rooij NF. J Micromechanics Microengineering. 2007; 17:R50–R80.
7. Park K. J Controlled Release. 2014; 190:3–8.
8. Elman NM, Ho Duc HL, Cima MJ. Biomed Microdevices. 2009; 11:625–631. [PubMed: 19169826]
9. Amar A, Kouki A, Cao H. Sensors. 2015; 15:28889–28914. [PubMed: 26580626]
10. Li, D., editor. Encyclopedia of Microfluidics and Nanofluidics. Springer New York; New York, NY: 2015.
11. Kwak R, Pham VS, Kim B, Chen L, Han J. Sci Rep. 2016; 6:25349. [PubMed: 27158057]
12. Van der Heyden FH, Bonthuis DJ, Stein D, Meyer C, Dekker C. Nano Lett. 2006; 6:2232–2237. [PubMed: 17034089]
13. Ren Y, Stein D. Nanotechnology. 2008; 19:195707. [PubMed: 21825725]
14. Vermesh U, Choi JW, Vermesh O, Fan R, Nagarah J, Heath JR. Nano Lett. 2009; 9:1315–1319. [PubMed: 19265427]
15. Li L, Mo J, Li Z. Phys Rev Lett. 2015; 115:134503. [PubMed: 26451560]
16. Fine D, Grattoni A, Zabre E, Hussein F, Ferrari M, Liu X. Lab Chip. 2011; 11:2526–2534. [PubMed: 21677944]
17. Gupta, NK.; Gianchandani, YB. Micro Electro Mechanical Systems, 2008 MEMS 2008 IEEE 21st International Conference on. IEEE; 2008. p. 38-41.
18. Lee YK, Nam JM. Small. 2012; 8:832–837. [PubMed: 22271621]
19. Liu MC, Shih HC, Wu JG, Weng TW, Wu CY, Lu JC, Tung YC. Lab Chip. 2013; 13:1743. [PubMed: 23475014]
20. Amin R, Knowlton S, Hart A, Yenilmez B, Ghaderinezhad F, Katebifar S, Messina M, Khademhosseini A, Tasoglu S. Biofabrication. 2016; 8:022001. [PubMed: 27321137]
21. Heikenfeld J, Zhou K, Kreit E, Raj B, Yang S, Sun B, Milarcik A, Clapp L, Schwartz R. Nat Photonics. 2009; 3:292–296.
22. Xu, J.; Midorikawa, K.; Sugioka, K. Microfluidics, BioMEMS, and Medical Microsystems XII. Gray, BL.; Becker, H., editors. Vol. 8976. 2014. p. 89760J
23. Shintaku H, Nishikii H, Marshall LA, Kotera H, Santiago JG. Anal Chem. 2014; 86:1953–1957. [PubMed: 24499009]
24. Chronis N, Liu G, Jeong KH, Lee L. Opt Express. 2003; 11:2370. [PubMed: 19471346]
25. Wang X, Cheng C, Wang S, Liu S. Microfluid Nanofluidics. 2009; 6:145–162. [PubMed: 20126306]
26. Grattoni A, Fine D, Zabre E, Ziemys A, Gill J, Mackeyev Y, Cheney MA, Danila DC, Hosali S, Wilson LJ, et al. ACS Nano. 2011; 5:9382–9391. [PubMed: 22032773]
27. Yang SY, Yang JA, Kim ES, Jeon G, Oh EJ, Choi KY, Hahn SK, Kim JK. Acs Nano. 2010; 4:3817–3822. [PubMed: 20507175]
28. Sinha PM, Valco G, Sharma S, Liu X, Ferrari M. Nanotechnology. 2004; 15:S585.
29. Grattoni A, Gill J, Zabre E, Fine D, Hussain F, Ferrari M. Anal Chem. 2011; 83:3096–3103. [PubMed: 21434670]
30. Foldvari M, Bagonluri M. Nanomedicine Nanotechnol Biol Med. 2008; 4:183–200.
31. Ferrati S, Fine D, You J, De Rosa E, Hudson L, Zabre E, Hosali S, Zhang L, Hickman C, Bansal SS, et al. J Controlled Release. 2013; 172:1011–1019.
32. Ferrati S, Nicolov E, Bansal S, Zabre E, Geninatti T, Ziemys A, Hudson L, Ferrari M, Goodall R, Khera M, et al. Adv Healthc Mater. 2015; 4:446–451. [PubMed: 25274059]
33. Taghipoor M, Bertsch A, Renaud P. Phys Chem Chem Phys. 2015; 17:4160–4167. [PubMed: 25564382]
34. Sparreboom W, van den Berg A, Eijkel JCT. Nat Nanotechnol. 2009; 4:713–720. [PubMed: 19898499]

35. Veenhuis RB, van der Wouden EJ, van Nieuwkasteele JW, van den Berg A, Eijkel JC. Lab Chip. 2009; 9:3472–3480. [PubMed: 20024025]
36. Nam SW, Rooks MJ, Kim KB, Rossnagel SM. Nano Lett. 2009; 9:2044–2048. [PubMed: 19397298]
37. Uemura T, Ono Y, Hijikata Y, Kitagawa S. J Am Chem Soc. 2010; 132:4917–4924. [PubMed: 20225869]
38. Ali M, Bayer V, Schiedt B, Neumann R, Ensinger W. Nanotechnology. 2008; 19:485711. [PubMed: 21836318]
39. Yameen B, Ali M, Neumann R, Ensinger W, Knoll W, Azzaroni O. Nano Lett. 2009; 9:2788–2793. [PubMed: 19518086]
40. Nunes SP, Behzad AR, Hooghan B, Sougrat R, Karunakaran M, Pradeep N, Vainio U, Peinemann KV. ACS Nano. 2011; 5:3516–3522. [PubMed: 21504167]
41. Fornasiero F, In JB, Kim S, Park HG, Wang Y, Grigoropoulos CP, Noy A, Bakajin O. Langmuir. 2010; 26:14848–14853. [PubMed: 20715879]
42. Karnik R, Fan R, Yue M, Li D, Yang P, Majumdar A. Nano Lett. 2005; 5:943–948. [PubMed: 15884899]
43. Peng R, Li D. Nanoscale. 2016; 8:12237–12246. [PubMed: 27256765]
44. Hoshyargar V, Ashrafizadeh S Nezameddin, Sadeghi A. ELECTROPHORESIS. 2016; 37:809–817. [PubMed: 26995195]
45. Haywood DG, Harms ZD, Jacobson SC. Anal Chem. 2014; 86:11174–11180. [PubMed: 25365680]
46. Khair AS, Squires TM. Phys Fluids. 2009; 21:042001.
47. Yossifon G, Mushenheim P, Chang YC, Chang HC. Phys Rev E. 2009; 79:046305.
48. Bruno G, Geninatti T, Hood RL, Fine D, Scorrano G, Schmulen J, Hosali S, Ferrari M, Grattoni A. Nanoscale. 2015; 7:5240–5248. [PubMed: 25707848]
49. Guan W, Fan R, Reed MA. Nat Commun. 2011; 2:506. [PubMed: 22009038]
50. Swain M. J Chem Inf Model. 2012; 52:613–615.
51. Chobanian AV, Bakris GL, Black HR, Cushman WC, Green LA, Izzo JL, Jones DW, Materson BJ, Oparil S, Wright JT, et al. Hypertension. 2003; 42:1206–1252. [PubMed: 14656957]
52. Cruickshank J, Thorp J, Zacharias FJ. The Lancet. 1987; 329:581–584.
53. Ainslie KM, Tao SL, Popat KC, Daniels H, Hardev V, Grimes CA, Desai TA. J Biomed Mater Res A. 2009; 91:647–655. [PubMed: 18988278]

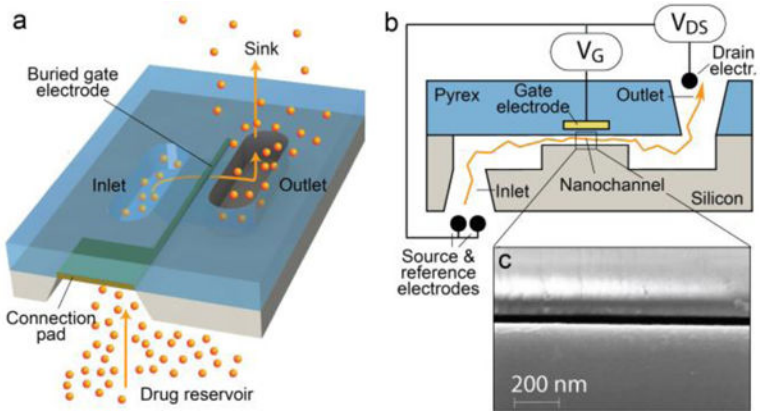

Fig. 1.

Schematic (a), cross-section (b), and SEM (c) image of the silicon membrane nanochannel substrate.

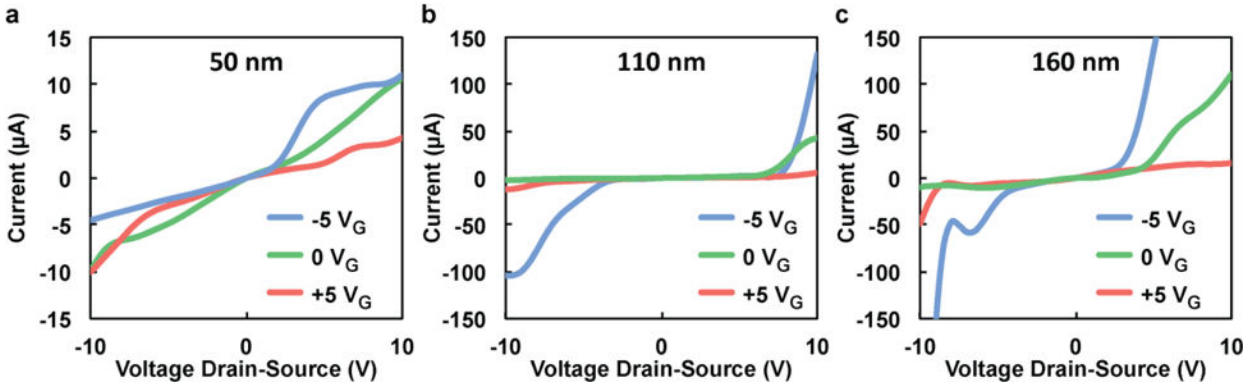

Fig. 2.

Drain-Source current as a function of voltage for IFET devices with (a) 50, (b) 110, and (c) 160 nm nanochannel membranes and 1 mM KCl electrolyte solution at different gate voltages (V_G).

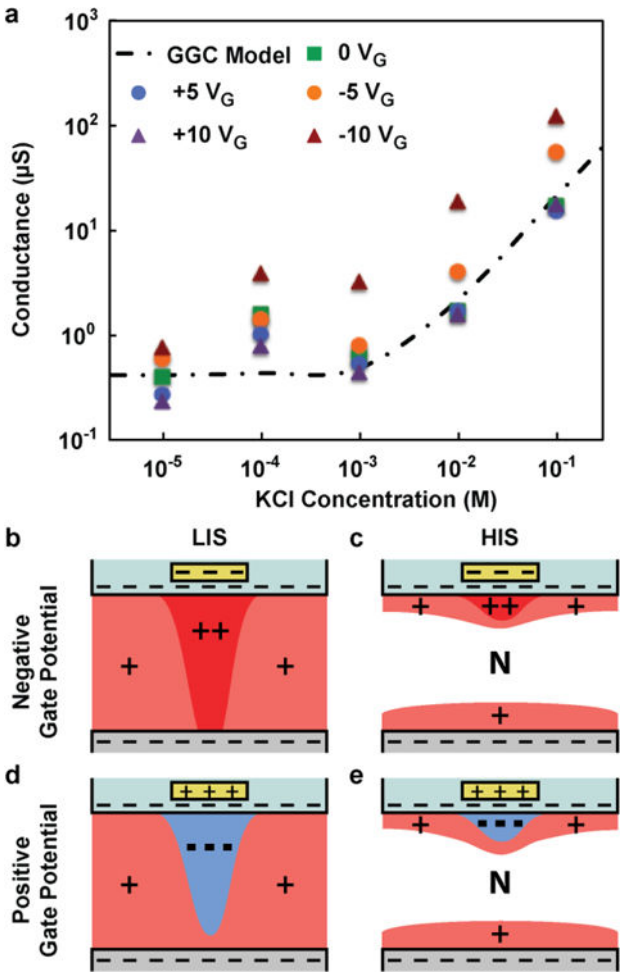

Fig. 3.

(a) Nanochannel conductance as function of KCl concentration for various gate voltages (symbols) and the Geometry-Governed-Conductance (GGC) model (dashed line). (b–e) Illustration of ions rearrangement for both negative (b,c) and positive (d,e) gate potential at low (b,d) and high (c,e) ionic strength (LIS and HIS respectively). N represents the neutral region.

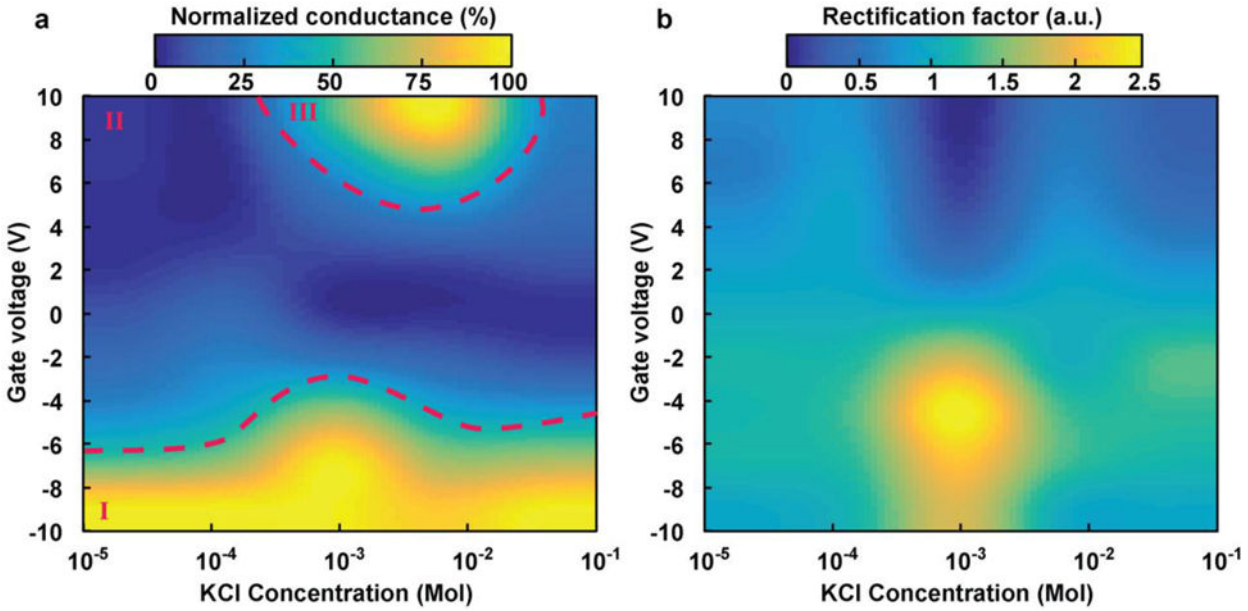

Fig. 4.

Heat maps to graphically represent (a) normalized conductance and (b) rectification at various gate voltages and KCl concentrations for a silicon membrane employing 50 nm nanochannels.

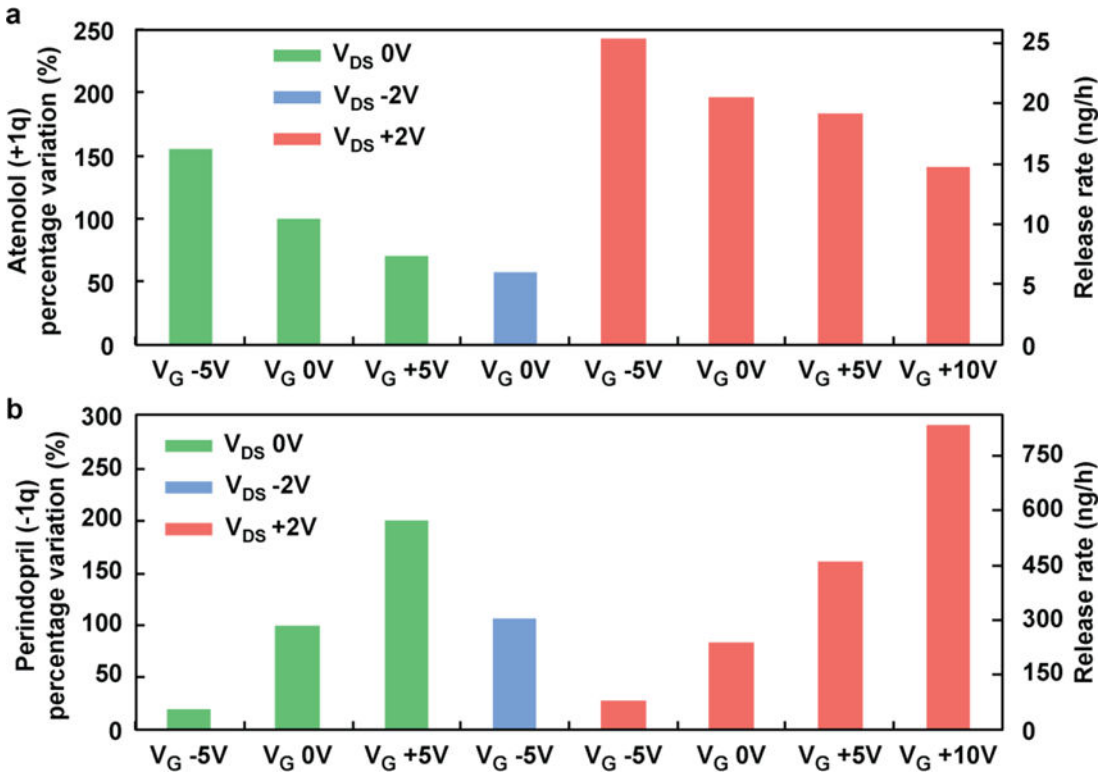

Fig. 5.

Percentage variation for two charged small molecules (a) atenolol and (b) perindopril at varying drain-source and gate voltages.